Hidden Charge-Density-Wave Order in a Low-T_c Superconductor 2*H*-$NbSe_2$

T. Kiss,[1] T. Yokoya,[1] A. Chainani,[2,3] S. Shin,[1,3] T. Hanaguri,[4] M. Nohara,[4] and H. Takagi[4]

[1]*Institute for Solid State Physics (ISSP), University of Tokyo, Kashiwa 277-8581, Japan*

[2]*Institute for Plasma Research, Bhat, Gandinagar-382 428, India*

[3]*The Institute of Physical and Chemical Research (RIKEN), Sayo-gun, Hyogo 679-5143, Japan*

[4]*Department of Advanced Materials Science, University of Tokyo, Tokyo 113-0033, Japan*

The Charge-density-wave(CDW) in 2*H*-$NbSe_2$(T_{CDW} ~ 33 K), which coexists with superconductivity(T_c = 7.2 K), is investigated using Angle-resolved photoemission spectroscopy as a function of temperature. Across T_{CDW}, energy and momentum(*k*) distribution curves show changes associated with the primary and secondary CDW vectors. The CDW is hidden, occurring at specific *k*-points on Fermi surfaces(FSs) in the 2-dimensional Brillouin zone(2D BZ) with spectral weight suppression, but no gap formation. The study rules out nesting between parallel sections of FSs in the 2D BZ and the van Hove singularity(vHs) driven CDW transition in 2*H*-$NbSe_2$, but spectral changes at the vHs stabilize the CDW.

PACS: 71.18.+y ; 71.45.Lr ; 79.60.-I

Fermi surface(FS) nesting in quasi one-dimensional(1D) and two-dimensional(2D) systems is believed to be intimately related to the seemingly competitive Charge-density-wave(CDW) order and superconductivity. CDW order occurs in many low dimensional materials such as quasi-1D $NbSe_3$, organic salts, quasi-2D transition-metal dichalcogenides(TMDs), etc [1,2]. It can occur without or with spin-density-wave(SDW) order or antiferromagnetism as in the high-T_c cuprates[2-4]. Separating out effects due to CDW or SDW and superconductivity, if possible, particularly in the high-T_c cuprates[3-5], is an extremely important requirement to understand material properties. Of course, in the limiting cases, materials are known to exhibit either localized charge carriers or supercurrents, and typify the difficulty.

In a CDW transition induced by FS nesting, a new charge periodicity is accompanied with lattice distortion characterized by $2k_F$, where k_F is the Fermi momentum, leading to the formation of a CDW gap at k_F [1]. Angle-resolved photoemission spectroscopy (ARPES) is uniquely suitable to measure the FS topology as well as the energy(ω)-, momentum(*k*)- and temperature(*T*)-dependent electronic structure of low-dimensional systems[6-8]. In particular, FS nesting and the resulting CDW gap formation have been successfully confirmed in quasi-1D systems with ARPES[8]. While the nesting can be nearly perfect in quasi-1D systems having parallel FS sheets, even for quasi-2D materials, parallel sections of FS sheets play an important role in modifying electronic properties[1,2,6,7]. ARPES studies of layered 2*H*-type TMDs which exhibit CDW order and low-T_c superconductivity have provided important aspects of their electronic structure. However, the mechanism of the incommensurate CDW transition in 2*H*-$NbSe_2$ (T_{CDW} ~ 33 K) coexisting with superconductivity(T_c = 7.2 K) has not been resolved yet . Possible candidates include a simple FS nesting [9], FS nesting with strong electron-phonon coupling effects[10,11], and the van Hove singularity(vHs) or saddle point driven CDW[12]. A direct clue to the CDW mechanism is to measure the CDW gap, or the CDW induced electronic structure changes, but previous ARPES studies of 2*H*-$NbSe_2$ [13-15] could not detect them due to the small changes inferred from transport experiments [16], and/or due to sample quality which influences the CDW transition [17]. Surprisingly, the superconducting gap was measured to show FS sheet dependence[18] with the achieved experimental resolution, although it is expected to be much smaller in magnitude than the CDW gap (since T_c = 7.2 K << T_{CDW} ~ 33 K).

In this letter, we present ARPES studies of high quality single crystal 2*H*-$NbSe_2$ (residual resistivity ratio (RRR) ~ 100), which exhibits *T*-dependent changes across T_{CDW} at special points in the Brillouin zone (BZ). The present ARPES results provide direct evidence ruling out nesting in the 2D BZ and the vHs driven CDW transition in 2*H*-$NbSe_2$, but spectral changes at the vHs aid the CDW. The energy and momentum-distribution curves (EDCs and MDCs) show changes in very good accord with the primary and secondary CDW vectors, across T_{CDW} ~ 33 K. The CDW is hidden, occurring at only specific *k*-points with spectral weight suppression, but no gap formation, consistent with earlier results. The result demonstrates the importance of *k*-dependent electron-phonon coupling and related changes in electronic structure for the CDW.

High quality single crystals of 2*H*-$NbSe_2$ with improved RRR of 100 were grown using the iodine vapor transport method [17]. *T*-dependent resistivity of a sample taken from the same batch as used for ARPES studies is plotted in Fig. 1. Inset a shows the low temperature region on an enlarged scale. The pronounced

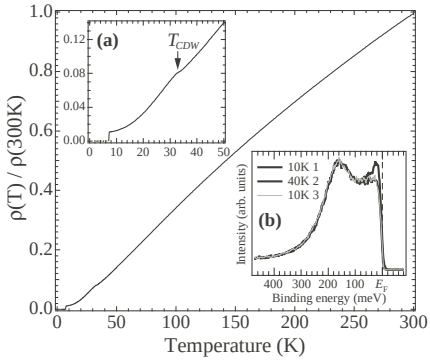

Fig. 1. *T*-dependent resistivity of single crystal 2*H*-$NbSe_2$ showing a residual resistivity ratio of 100, confirming the high quality. Inset a emphasizes the changes across T_{CDW}. Inset b shows a sequence(1-2-3) of *T*-cycling (10K-40K-10 K) ARPES spectra across T_{CDW} at a Fermi vector (same as spectra at **d** in Fig. 3c), demonstrating very high reproducibility of the spectral changes.

hump structure around 33 K corresponds to the CDW transition and is clearly visible in samples with RRR=100 compared to samples with RRR~30, indicating enhancement of the CDW in the higher RRR samples [17]. X-ray Laue diffraction patterns were used to mount samples for desired orientations, which were further confirmed by the symmetry of the ARPES spectra. The ARPES measurements were performed on a spectrometer built using a hemispherical electron analyzer (GAMMADATA-SCIENTA SES2002) and a high-flux He discharging lamp with a toroidal grating monochromator. The spectra were measured with He Iα resonance line (21.218eV) at a vacuum of ~ 1 x 10^{-10} Torr during measurements and a base vacuum of < 5 x 10^{-11} Torr. The total energy resolution (analyzer and light) was set to 8.0 meV. The angular resolution was set to 0.18° corresponding to *k*-resolution of 0.0067 $Å^{-1}$. Normalization of spectra was done with scan time [19]. We attribute our reliably detecting small but important CDW induced electronic structure change to no degradation in spectra obtained on temperature cycling across T_{CDW}. As seen for a typical Fermi surface crossing in inset b to Fig 1, highly reproducible spectra were obtained in every case on temperature cycling. Clean surfaces were obtained by cleaving samples *in-situ*. Samples were cooled using a liquid helium continuous flow cryostat and sample temperatures were measured using silicon-diode sensors. The Fermi level (E_F) of samples was referenced to that of a gold film evaporated onto the sample substrate and its accuracy is estimated to be better than ± 0.2 meV.

Figures 2a and b are ARPES intensity maps obtained from measured EDCs, integrated within ± 6 meV of E_F, at 40 K (normal phase) and 10 K (CDW phase), respectively. At 40 K, we observe high-intensity curved regions that correspond to two FS sheets around the Γ(A) point and two around the K(H) point, as discussed below. The vHs, or the saddle point, is located along the Γ(A)-K(H) high symmetry line, in between the larger FS sheets around Γ(A) and K(H). By comparing with band structure calculations [20-22], the FS sheets around Γ(A) and K(H) can be ascribed to the cylindrical double-walled FS sheets along the Γ-A and K-H lines derived

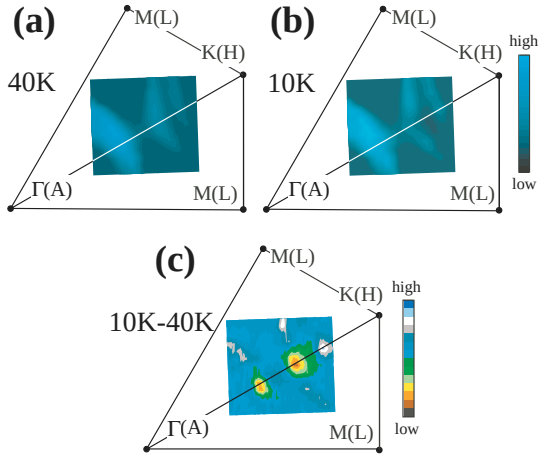

Fig. 2. (a) and (b), ARPE intensity maps at E_F (energy window = E_F ± 6 meV) of 2*H*-$NbSe_2$ at 40 K (normal phase) and 10 K (CDW phase), respectively. The wedge shows one sixth of the first BZ. (c) Difference intensity map (b-a) in *k*-space between 40 and 10 K, showing two special spots with significant intensity reduction in the CDW phase.

from Nb 4*d* orbitals. The incommensurate CDW phase (10 K) intensity map exhibits clear modifications in intensity and shape of the FSs when compared with the normal-phase (40 K). The larger FS sheet around K(H) loses intensity along Γ(A)-(H) while the shape of the smaller FS sheet around K(H) also changes in curvature along Γ(A)-(H). In order to emphasize the electronic structure changes at E_F, we have subtracted the intensity map at 40 K from that at 10 K, as shown in Fig. 2c. *T*-dependent changes give rise to two low intensity pits or spots along the Γ(A)-K(H) line on both sides of the vHs, indicating that the electronic-structure changes across the CDW transition mainly occurs at spots, and not along extended regions on FS sheets in the 2D BZ as expected from the conventional nesting scenario for CDW transitions. Thus, along the Γ(A)-K(H) direction, the map identifies two special spots where a significant reduction in intensity is observed, coupled with small intensity increase at other *k*-points.

The modification of intensity at E_F across T_{CDW} is seen in more detail in the *T*-dependent MDCs at E_F. Figure 3a shows MDCs measured along 13 cuts in the BZ shown in Fig. 3b obtained from the data used for the FS mappings of Figs. 2a and b. We now observe fine electronic structures and their *T*-dependence more clearly. For example, the two FS sheets around Γ(A) are clearly evident from the peak and shoulder structures of the MDCs from 8th to 13th cuts. From the *T*-dependence, it is understood that intensity reduction at 10 K along the Γ(A)-K(H) direction shown in Fig. 2c results from changes in Γ2 and K2 sheets centered at Γ(A) and K(H), respectively (see Fig.4 for identifications of FS sheets: Γ1,Γ2,K1 and K2). In addition, the peak position of the K1 FS sheet shifts, leading to the change in FS curvature seen in Fig. 2b. In Figs. 3c and d, we show *T*-dependent EDCs at selected points in the BZ (**a** to **e** in Fig. 3a) plotted over a wider energy region, and near E_F region, respectively. The EDCs at **a** show *T*-dependent changes just near E_F, which are more evident in Fig. 3d and the increase at 10 K can be explained by the change of the Fermi-Dirac distribution function. In contrast, in the EDCs at **b**, **c** and **d**, peak intensity upto ~ 80 meV decreases as *T* decreases. At point **b**, close location of the

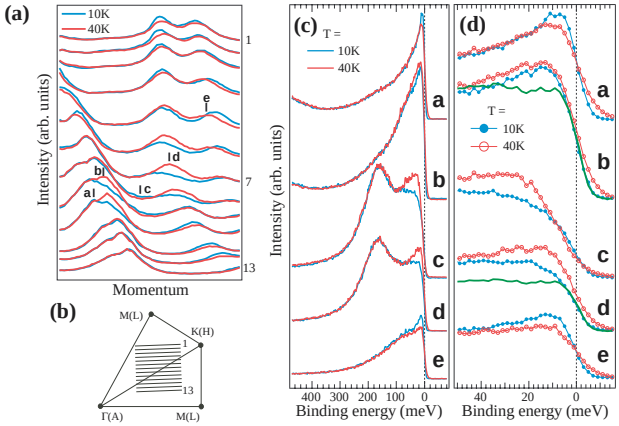

Fig. 3. (a) *T*-dependent MDCs measured along 13 cuts in the BZ as shown in (b). (c) *T*-dependent EDCs measured at 5 points in the BZ, showing the changes at the FS crossings **a**, **b**, **d** and **e** along the Γ-K direction on Γ1, Γ2, K1 and K2 FSs, as well as at **c**, the vHs known in 2*H*-$NbSe_2$. (d) Enlargement of the region near E_F of (c), with the green curves showing the Fermi edge of gold.

17th and 18th bands (as named in ref. 22) constituting the Γ1 and Γ2 FSs makes it difficult to identify the change in the 18 th band alone. On the other hand, changes in EDCs at **c** and **d** are rather clear. We also find that though the spectral-shape change over a wider energy region is larger at **c** (which corresponds to the location of the vHs) than at **b** and **d**, the intensity at E_F decreases only at **b** and **d** across T_{CDW}, as seen in the *T*-dependent changes of the FS mapping (Fig. 2c) and the MDCs (Fig. 3a). As is evident from the EDCs at **b** and **d**, the change across the CDW transition does not result in opening of a gap, but reduction of intensity at E_F [23]. Similar reduction in *T*-dependent spectra has been observed in 2*H*-$TaSe_2$ only for K-centered FSs and ascribed to CDW gap formation [14,24]. At **e**, *T*-dependent changes near E_F is similar to that at **a** with increase in spectral intensity, and opposite in behavior compared to **b**, **c** and **d**. The present results indicate that the CDW transition primarily causes modifications of the 18th band upto ~ 80 meV binding energy and reduces the spectral weight at E_F dominantly at the spots on the Γ2 and K2 FS sheets. Note that the energy scale of 80 meV is slightly larger than the observed depletion in momentum averaged tunneling spectra, which was ascribed to the CDW formation[25].

A symmetrization of the two spots shown in Fig. 2c in the BZ (red and blue circles in Fig. 4a) leads to a direct relation of these special *k*-points with the CDW vectors known from neutron[26] and X-ray diffraction[27] studies of 2*H*-$NbSe_2$. The red spots are primary CDW vectors(q_1,q_2,q_3) (=0.68±0.03ΓM=0.34a^* (a^*=4π/($3^{0.5}a$))) and the blue spots are secondary CDW vectors (=0.98±0.03ΓK) corresponding to ($q_i \pm q_j$) with *i, j* = 1, 2, 3, consistent with the direction and magnitude (= 0.694 $Å^{-1}$ = 0.671ΓM=0.33a^*) for the CDW vector known from diffraction studies[26,27]. The obtained FSs [15,18] are shown as green curves in Fig 4a (labeled Γ1, Γ2 for the smaller and larger FSs centered around the Γ(A) point, and similarly, K1 and K2 around the K(H) point), consistent with band structure calculations[20-22]. The magnitude in *k*-space between parallel sections of the hexagonal FS sheets around the Γ(A) point (0.886$Å^{-1}$ = 0.84ΓM=0.42a^*) is much larger than the known CDW vector[26,27]. The primary vectors form a triangle in *k*-space(red circles on FS K2), while the secondary vectors (blue circles on FS Γ2) lie on the Kagome lattice(thin gray lines), corresponding to a 'hidden' CDW order in the hexagonal lattice. We use the term 'hidden' to represent the result that parallel sections of measured Fermi surfaces do not match the known CDW vector as believed earlier[13], but the CDW affected regions are hidden in the same Fermi surfaces[28]. The observed electronic-structure changes across T_{CDW} of 2*H*-$NbSe_2$ are consistent with the neutron diffraction study which discovered the coexistence of superconductivity and the CDW phase, and also speculated on the role of multiple scattering from primary CDW vectors due to observation of additional spots. The present ARPES results thus confirm the validity of multiple scattering by identifying the *k*-points affected by the primary CDW vectors and the secondary CDW vectors. The result rules out models of FS nesting between parallel sections in the 2D hexagonal BZ. The present results also show that the CDW affected spots are different from the vHs, though we observe significant changes in the intensity at higher energy at the vHs. The spectral changes at the vHs would play an important role in stabilizing the CDW from the more generalized condensation energy point of view [29]. Since the vector connecting two vHs *k*-points is different from the known CDW vector, and, the energy position of the vHs is ~ 30 meV away from E_F, both of which are necessary conditions for the vHs scenario [12], it indicates that the CDW is not driven by the vHs although spectral changes at the vHs would certainly stabilize the transition. Another viewpoint is that the vHs acts like a negative scattering center and its removal would cause increase in conductivity below T_{CDW}[12]. While ARPES cannot distinguish between these scenarios, the CDW transition in 2*H*-$NbSe_2$ is weak as compared to a conventional CDW transition. From our results, we infer that CDW nesting is possible only between parallel lines consisting of special *k*-points lying along the k_z axis (Fig. 4b), since 2*H*-$NbSe_2$ exhibits negligible dispersion along the k_z axis for the K2 FS[15,22]. We believe the small warping of Γ2 and K2 FS sheets along k_z compared to Γ1 and K1[15,22], and the relatively small Fermi velocity (0.56eVÅ) of the 18th band on the K2 FS as compared to the K1 FS(with a larger Fermi velocity of 0.66 eVÅ) is important for the CDW. The strong electron-phonon coupling then leads to a peak in the generalized electronic susceptibility, leading to a dip(softening) in the Σ_1-mode phonon dispersion at [2/3(Γ-M)], which induces the CDW transition [10,11,24]. Note that the direction and magnitude of the primary vectors (q_1,q_2,q_3) match [2/3(Γ-M)], in agreement with neutron scattering results[26]. While the importance of *k*-dependent electron-phonon coupling has been discussed [10,11], and a recent study has also identified the K1 FS to have an anomalously high electron-phonon coupling constant[30], the CDW affected regions or the 'hot spots' lie on the Γ2 and K2 FS sheets.

The important difference that emerges between 2*H*-$TaSe_2$ and 2*H*-$NbSe_2$ is the energy position of the vHs : almost 0 meV for 2*H*-$TaSe_2$ [10]and ~30 meV for 2*H*-$NbSe_2$. Magnetic susceptibility of 2*H*-$TaSe_2$ and 2*H*-TaS_2 show a sudden reduction around the T_{CDW} with larger change in 2*H*-$TaSe_2$, while that of 2*H*-$NbSe_2$ has a broad maximum at low temperature [16]. The changes in FS topology also relate with the Hall coefficient changes as a function of *T* [31]. As for the metallicity in the CDW phase of 2*H*-$NbSe_2$, intensity of MDCs at E_F even for the

Γ2 and K2 FSs, other than at the CDW affected spots

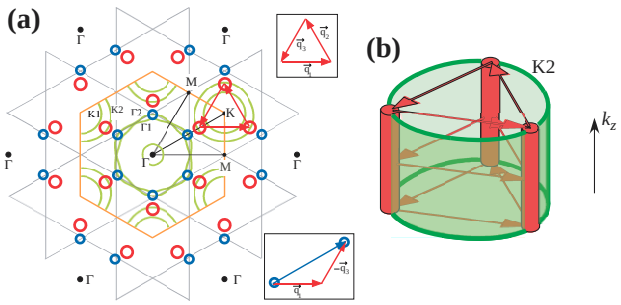

Fig.4. (a) Symmetric arrangement of the two spots (red and blue circles) in the BZ of 2*H*-$NbSe_2$. Orange-colored hexagon is the first BZ. FSs (green curves) are overlaid to show primary CDW vectors(q_1,q_2,q_3) lie on K2 and connect red circles, while blue circles connect secondary CDW vectors ($q_i \pm q_j$) with *i, j* = 1,2,3. (b) A schematic of FS K2 with red spots lying along k_z form parallel lines which are nested by primary CDW vectors.

in *k*-space, actually increase at lower temperatures representing so called 'cold-spots'(Fig. 2a and b). This suggests a reduction of the scattering at lower temperatures, consistent with the resistivity [31] and optical conductivity results [32]. A decreasing scattering rate below T_{CDW} in 2*H*-$TaSe_2$ for the Γ-centered FSs was shown to have good correspondence with the resistivity and Drude scattering rate [33,34]. In the present case, the opposite changes on Γ1 and K1 FSs compared to Γ2 and K2 FSs along the Γ-K direction, and also at different *k*-points on the Γ2 and K2 FSs across T_{CDW}, represent a separation of electrons in *k*-space responsible for the CDW formation and the surviving metallicity in the CDW phase. A similar picture was suggested by ARPES of 2*H*-$TaSe_2$ [33], X-ray studies on 2*H*-$NbSe_2$ [27] and optical spectroscopy studies of 2*H*-$TaSe_2$ and 2*H*-$NbSe_2$ which show increase in spectral weight at very low energy[32,34].

In conclusion, *T*-dependent ARPES of high quality 2*H*-$NbSe_2$ across the CDW transition shows evidence for a novel form of CDW order involving specific *k*-points in the 2D BZ. The EDCs and MDCs show coupled changes associated with the primary and secondary CDW vectors, across $T_{CDW} \sim 33$ K. The CDW is hidden, occurring at specific *k*-points with spectral weight suppression, but no gap formation. The study rules out nesting in the 2D BZ and the vHs driven CDW transition models in 2*H*-$NbSe_2$, although spectral changes at the vHs aid the CDW transition.

Acknowledgements: We thank Profs. K. Motizuki, N. Nagaosa, and M. Grioni for very valuable discussions. This work was supported by grants from the Ministry of Education, Culture and Science of Japan. T.K. thanks the Japan Society for the Promotion of Science for financial support.

References

[1] G. Gruner, Density Waves in Solids (Addison-Wesley, Massachusetts, 1994).
[2] A. M. Gabovich, A. I. Voitenko and M. Ausloos, Phys. Reports, **367**, 583(2002).
[3] J.M. Tranquada et al. Nature **375**, 561 (1995).
[4] J. Orenstein and A.J. Millis, Science **288**, 468(2000); and references therein.
[5] X.J. Zhou et al. Science **286**, 268 (1999); J.E. Hoffman *et al*. Science **295**, 466(2002); C. Howald *et al*. Phys Rev B **67**, 014533(2003).
[6] B. Dardel *et al*., Phys. Rev. B **45**, 1462-1465 (1992) ; G. H. Gweon *et al*. Phys. Rev. Lett. **81**, 886(1998) ; M. Hengsberger et al. , Phys. Rev. Lett. **83**, 592 (1999) ; L. Perfetti *et al*. Phys. Rev. Lett. **90**, 166401(2003).
[7] A. Lanzara *et al*. *Nature* **412,** 510 (2001) ; A. Kaminski *et al*., *Nature* **416,** 610 (2002) ; T. Valla *et al*., *Nature* **417,** 627 (2002).
[8] K. E. Smith *et al*., Phys. Rev. Lett. **70**, 3772 (1993) ; K. Breuer *et al*., Phys. Rev. Lett. **76**, 3172 (1996) ; J. Schäfer *et al*. Phys. Rev. Lett. **91**, 066401 (2003).
[9] J. A. Wilson, Phys. Rev. B **15**, 5748 (1977).
[10] N. J. Doran *et al*., J. Phys. C **11**, 699 (1978).
[11] Y. Nishio, M. Shirai, N. Suzuki, and K. Motizuki, J. Phys. Soc. Jpn. **63**, 156 (1994).
[12] T. M. Rice and G. K. Scott, Phys. Rev. Lett. **35**, 120 (1975).
[13] Th. Straub *et al.*, Phys. Rev. Lett. **82**, 4504 (1999).
[14] R. Liu, C. G. Olson, W. C. Tonjes, and R. F. Frindt, Phys. Rev. Lett. **80**, 5762 (1998); R. Liu *et al*., Phys. Rev B **61**, 5212 (2000); W. C. Tonjes *et al*., Phys. Rev. B **63**, 235101 (2001).
[15] K. Rossnagel et al., Phys. Rev. B **64**, 235119 (2001).
[16] C. Ayache, R. Currat, B. Hennion, and P. Molinie, Journal de Physique IV, Colloque C2, supplement au Journal de Physique I, 3 125 (1993).
[17] K. Iwaya et al., Physica B (in press).
[18] T. Yokoya *et al*. Science **294**, 2518(2001).
[19] Normalization with scan time using a He discharging lamp at constant power, is the same as normalization with photon flux when using a synchrotron source.
[20] L. F. Mattheiss, Phys. Rev. B **8**, 3719 (1973).
[21] G. Wexler and A. M. Woolley, J. Phys. C **9**, 1185 (1976).
[22] R. Corcoran *et al*., J. Phys. Condens. Matter **6**, 4479 (1994); H. Harima, private communication.
[23] One other possibility is that since the CDW vector connects only specific points in the 2D BZ, a finite momentum resolution intrinsic to a measurement can wipe out the CDW gap.
[24] B. Dardel et al., J. Phys. Condens. Matter **5**, 6111 (1993).
[25] C. Wang et al., Phys. Rev. B **42**, 8890 (1990) ;H. F. Hess et al., J. Vac. Sci. Technol. **8**, 450 (1999).
[26] D. E. Moncton, J. D. Axe, and F. J. DiSalvo, Phys. Rev. Lett. **34**, 734 (1975); Phys. Rev. B **16**, 801(1977).
[27] C. H. Du et al., J. Phys. Cond. Matter **12**, 5361(2000).
[28] M.-H. Whangbo et al., Science 252, 96 (1991); K. Smith et al., Phys Rev Lett. 76, 3172(1996)
[29] M.R. Norman et al., Phys. Rev. B **61**, 14742 (2000).
[30] T. Valla et al. cond-mat/0308278.
[31]M. Naito and S. Tanaka, J. Phys. Soc. Jpn. 51, 219 (1982); T. W. Jing and N. P. Ong
Phys. Rev. B **42**, 10781-10784 (1990); N. P. Ong, Phys. Rev. B **43**, 193 (1991).
[32] S.V. Dordevic et al., Phys. Rev. B **64**, 161103(R) (2001); Eur. J. Phys. B **33**, 15(2003).
[33] T. Valla et al., Phys. Rev. Lett. **85**, 4759 (2000).
[34] V. Vescoli, L. Degiorgi, H. Berger, and L. Forró, Phys. Rev. Lett. **81**, 453 (1998).